JPEDAV (2006) 27:333-342
DOI: 10.1361/154770306X116261
1547-7037/$19.00 ©ASM International

Study of Diffusion Mobility of Al-Zn Solid Solution

Y.W. Cui, K. Oikawa, R. Kainuma, and K. Ishida

(Submitted January 17, 2006; in revised form March 29, 2006)

Diffusion mobilities in binary Al-Zn solid solutions are critically assessed by fitting experimental diffusion data with a phenomenological model, called the DIffusion Controlled TRAnsformation (DICTRA) code. Good agreement is obtained with comprehensive comparisons between calculated values and experimental observations. With a thermodynamic description as the key input, the assessed mobility is further validated by three simulated diffusion experiments, that is, one semi-infinite vapor-solid diffusion couple and two long cylindrical diffusion couples.

Keywords aluminum alloys, binary diffusion, critical assessment, DICTRA modeling, diffusivity coefficient

1. Introduction

Hot-dip galvanizing is widely used in automotive and other industries. It is a basic process in which diffusion kinetics play a major role. Thus, understanding of diffusion characteristics of industrially important alloys such as those of the Al-Fe-Zn system are highly relevant and have attracted much attention through the years. In these alloys, diffusion processes govern the kinetics of galvanizing and, hence, ultimately control the properties and stability of the galvanizing layers. The Al-Zn system is a binary boundary of the ternary Al-Fe-Zn system and is also the classic metal system for studies of spinodal decomposition. This binary system has a fairly symmetric equilibrium miscibility gap bounded by simple face-centered-cubic (fcc) substitutional alloy phases with similar lattice constants.

Knowledge of both thermodynamic and diffusional characteristics of the Al-Zn system is of critical importance in developing an understanding of the Al-Fe-Zn system. To accomplish this, an advanced computational technique is an appropriate underlying tool. So far, the CALPHAD technique has made significant progress, and a wide variety of multicomponent thermodynamic databases have already been constructed. Thus there is no longer a problem in finding appropriate thermodynamic descriptions for specific alloy systems. For instance there are three[1-3] for the Fe-Zn system and two[4,5] for the Al-Zn system. Unfortunately, this is not the case for diffusion data, though Du et al.[6] have recently reported a least-squares analysis of the impurity diffusion of Zn in fcc Al. In contrast, as practical algorithms, with the phase field model representing one example, move toward maturity, these algorithms can be applied to describe kinetic behavior with equations that describe variable mobilities.[7,8] Such algorithms can at present realistically model microstructural evolution with input of real material parameters.[9,10] As a consequence, there is an increasing need for determination of adequately accurate expressions of diffusion data sets to supplement purely thermodynamic approaches. An extension of the CALPHAD approach has been developed, is known as the DIffusion Controlled TRAnsformation (DICTRA) code, and operates under the CALPHAD framework.

This code is capable of simulating diffusion data to model diffusion-limited phenomena for multicomponent alloys. Accordingly, the purpose of the present work is to assess the atomic mobilities in the Al-Zn solid solution on the basis of plentifully available experimental data and to provide insight into diffusion characteristic with simulation of diffusion profiles by applying the assessed mobility parameters.

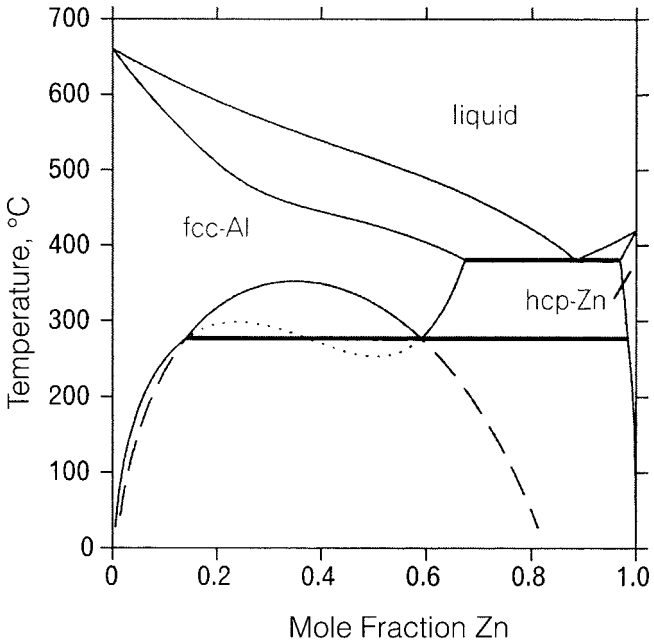

Fig. 1 Calculated Al-Zn phase diagram with the selected parameters from the thermodynamic description[5]

Y.W. Cui, Department of Materials Science, Graduate School of Engineering, Tohoku University, Sendai 980-8579, Japan; **K. Oikawa, R. Kainuma,** and **K. Ishida,** Department of Materials Science, Graduate School of Engineering, Tohoku University, Sendai 980-8579, Japan, and Core Research for Evolutional Science and Technology (CREST), Japan Science and Technology Agency (JST). Contact e-mail: ycui@material.tohoku.ac.jp.

Table 1 Frequency factors, activation energies, and other experimental information of the tracer diffusion coefficients in Al and Al-Zn alloys

Reference	Q, kJ/mol	D_o, cm^2/s	T, °C	Data type	Method
Hilliard et al.[15]	129.4	1.1	400-650, 325-610	D_{Zn}^{Al} $D_{Zn}^{Al,Zn}$	Tracer sectioning
Ceresara et al.[16]	127.4	0.9	403-559	D_{Zn}^{Al}	Resistometric method
Stoebe et al.[17]	127.5	0.1	330-460	D_{Al}^{Al}, $D_{Al}^{Al,Zn}$	Nuclear magnetic resonance (NMR)
Chatterjee et al.[18]	163.0	400	350-485	D_{Zn}^{Al}, $D_{Zn}^{Al,Zn}$	Tracer sectioning
Peterson et al.[19]	120.8	0.259	357-653	D_{Zn}^{Al}	Tracer sectioning
Godeny et al.[20]	121.4	0.30	315-650	D_{Zn}^{Al}, $D_{Zn}^{Al,Zn}$	Tracer sectioning
Fujikawa et al.[21]	118.1	0.17	165-645	D_{Zn}^{Al}, $D_{Zn}^{Al,Zn}$	Residual activity
Beke et al.[22]	120.3	0.27	360-660	D_{Zn}^{Al}, $D_{Zn}^{Al,Zn}$	Tracer sectioning
Erdelyi et al.[23]	120.6	0.20	377-630	D_{Zn}^{Al}	Electrical resistance
Cermak et al.[24]	…	…	312-509	$D_{Zn}^{Al,Zn}$	Residual activity
Godeny et al.[25]	…	…	255.7-510	$D_{Zn}^{Al,Zn}$	Tracer sectioning
Nicholls et al.[26]	117.9	0.27	110-160	D_{Zn}^{Al}	Analysis of grain boundary composition profile
Varadarajan et al.[27]	112	0.018	180-235	D_{Zn}^{Al}	Analysis of grain boundary composition profile

Table 2 Self-diffusions of Zn and Al

Reference	Q, kJ/mol	D_o, cm^2/s	T, °C	Data type	Method
Lundy and Murdock[28]	142.4	1.7	450-650	D_{Al}^{Al}	Tracer sectioning
Stoebe et al.[17]	127.5	0.10	330-500	D_{Al}^{Al}	NMR
Beyeler and Adda[29]	144.4	…	400-610	D_{Al}^{Al}	Tracer sectioning
Volin and Balluffi[31]	126.4	0.176	85-209	D_{Al}^{Al}	TEM on voids
Messer et al.[30]	123.5	0.137	510-780	D_{Al}^{Al}	NMR
Hilliard et al.[15]	85.8	0.031	325-405	D_{Zn}^{Zn}	Tracer sectioning
Shirn et al.[33]	101.7 (pe)	0.58 (pe)	240-410	D_{Zn}^{Zn}	Tracer sectioning
	91.3 (pa)	0.13 (pa)			
Batra[34]	…	…	352-412	D_{Zn}^{Zn}	Tracer sectioning
Peterson and Rothman[35]	96.3 (pe)	0.18 (pe)	240-418	D_{Zn}^{Zn}	Tracer sectioning
	91.7 (pa)	0.13 (pa)			
Chhabildas and Gilder[36]	…	…	300-400	D_{Zn}^{Zn}	Tracer sectioning

NMR, nuclear magnetic resonance; TEM, transmission electron microscopy; pe, perpendicular to the hexagonal *c*-axis; pa, parallel with the hexagonal *c*-axis

2. Modeling

A thermodynamic description of the Al-Zn system has been well established.[5] The calculated phase diagram based on the thermodynamic description is reproduced in Fig. 1. In the sections that follow, attention will focus on diffusion analysis of this system.

2.1 Modeling of Mobility

Andersson and Agren[11] suggested that the atomic mobility M_B can be expressed as a function of temperature T:

$$M_B = M_B^0 \exp\left(\frac{-Q_B}{RT}\right)\frac{1}{RT} = \exp\left(\frac{RT\ln M_B^0}{RT}\right)\exp\left(\frac{-Q_B}{RT}\right)\frac{1}{RT} \quad \text{(Eq 1)}$$

where Q_B is the activation energy, M_B^0 is the frequency factor and R is the gas constant. Similar to the phenomenological CALPHAD concept, the parameter Ψ_B (M_B^0 or Q_B) is assumed to be a function of composition,[12-14] that can be expressed by a Redlich-Kister polynomial:

$$\Psi_B = \sum_i x_i \Psi_B^i + \sum_i \sum_{j>i} x_i x_j \left[\sum_{r=0}^{m} {}^r\Psi_B^{i,j}(x_i - x_j)^r\right] + \sum_i \sum_{j>i} \sum_{k>j} x_i x_j x_k \left[v_{ijk}^s {}^s\Psi_B^{i,j,k}\right], (s = i, j, k) \quad \text{(Eq 2)}$$

where x_i is the mole fraction of element i, Ψ_B^i is the value of Ψ_B for pure i, and $\Psi_B^{i,j}$ and $\Psi_B^{i,j,k}$ are binary and ternary interaction parameters, and the parameter v_{ijk}^s is given by $v_{ijk}^s = x_s + (1 - x_i - x_j - x_k)/3$. For a binary system, only the first two terms of the right-hand side remain. If tracer diffusion is defined as diffusion in a medium of gradient-free homogeneous composition (e.g., radioisotope movement in self-diffusion studies), the tracer diffusion coefficient is rigorously related to the atomic mobility by a simple relation

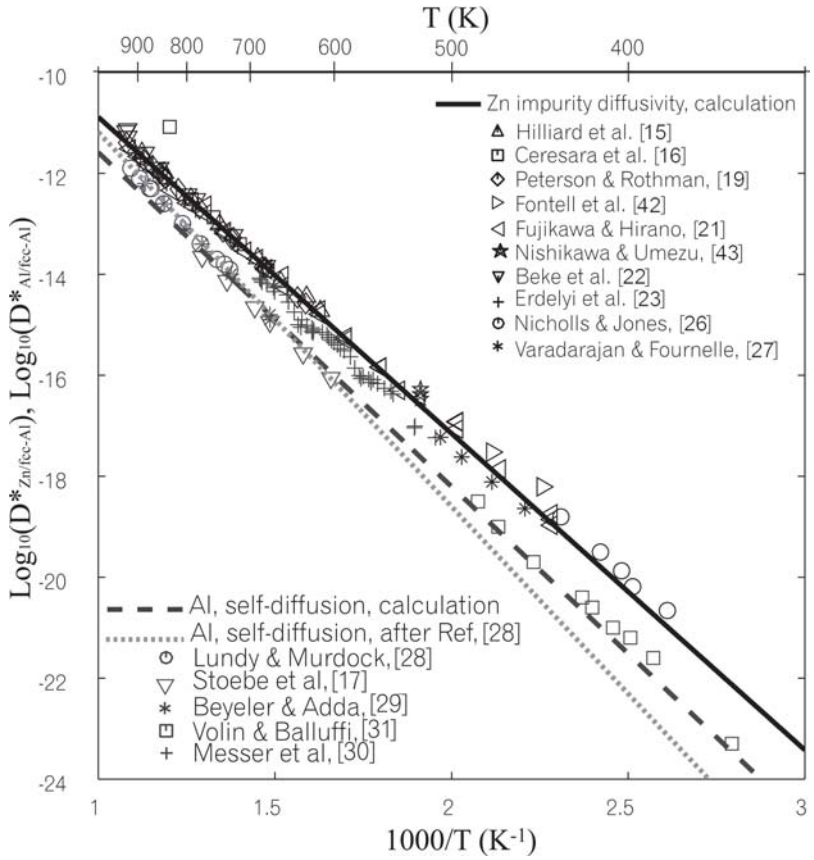

Fig. 2 Self-diffusion of the fcc-Al (broken line and black and gray markers) and impurity diffusivity of Zn in the fcc-Al (solid line and black and gray markers). The lines are calculated, and relevant experimental data points are plotted (the markers denote the experimental values). The dotted line is taken from Ref 28 for the fcc-Al self-diffusivity.

$D_k^* = RTM_k$. In comparison, if chemical diffusion is considered to be diffusion in the presence of compositional gradients, the effect of the gradients can be derived by including an accurate thermodynamic description of the material system:

$$\tilde{D}_{kj}^n = \sum_{i=1}^{n-1} (\delta_{ik} - x_k) x_i M_i \left(\frac{\partial \mu_i}{\partial x_j} - \frac{\partial \mu_i}{\partial x_n} \right) \quad \text{(Eq 3)}$$

where the Kronecker delta $\delta_{ik} = 1$ when $i = k$ and 0 otherwise, and μ_i is the chemical potential. With the proposed relations, the parameter Ψ_B can be numerically assessed by fitting to the experimental data, particularly the tracer diffusivity and chemical diffusion coefficient.

2.2. Experimental Information

Although extensive experimental studies have been made of diffusion phenomena in binary Al-Zn alloys, the present paper has no intention of being a critical review. Rather, data were selected for mobility assessment or for purposes of comparison with results from the present calculations. The criterion for selection of experimental data was the extent to which the results from different investigations agree among themselves or with the features of the evaluated Al-Zn phase relationships.

2.2.1 Tracer Diffusivity of Zn in Pure Al and in fcc Solid Solution. The amount of experimental data on the tracer diffusivity of Zn is quite abundant. Due to the limitation of the experimental technique, early studies were confined to relatively high temperatures,[15-25] whereas more recent efforts have extended measurements to lower temperatures.[26,27] References for the most relevant data are listed in Table 1 and include the experimental method, the data type, and the temperature range. It is apparent that the frequency factors and activation energies of the tracer diffusivity deduced from most of the listed resources roughly reconcile with each other over the entire range of temperature with the only exception being the work of Chatterjee and Fabian,[18] and this work was excluded from the assessment procedure.

2.2.2 Self-Diffusion of Al and Zn. The experimental information pertaining to self-diffusion data is relatively limited. Table 2 outlines the relevant experimental information.[15,17,28-31,33-36] The derived activation energy and frequency factor of Al self-diffusion, shown in the second and third columns, appear somewhat scattered. Engstrom and

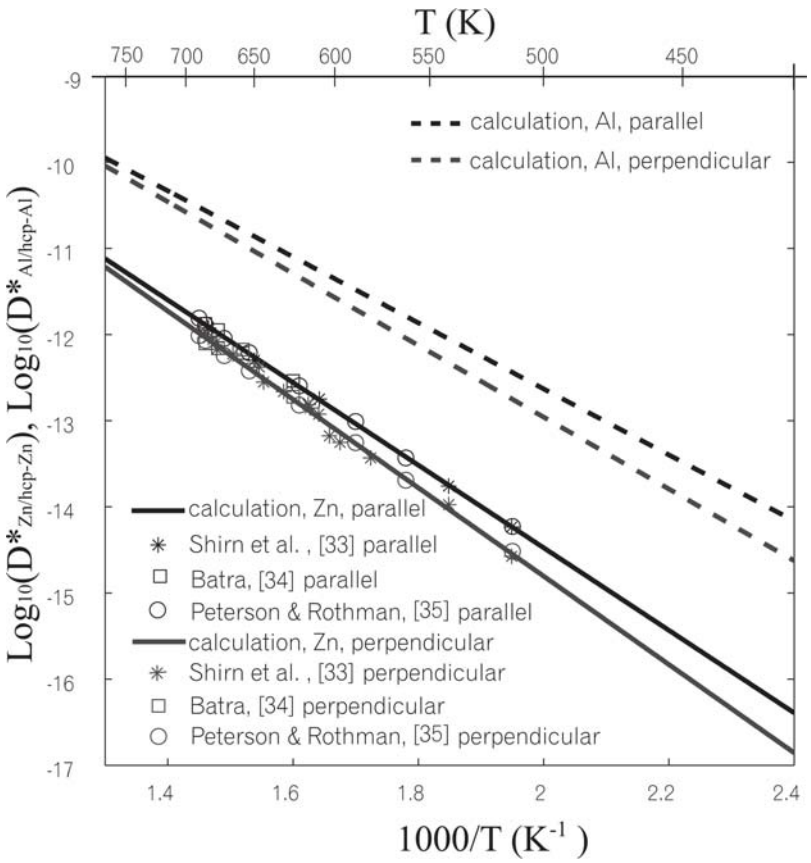

Fig. 3 Self-diffusivities of the cph-Zn and Al compared with the experimental points

Table 3 The optimized mobility in this work

Endpoint parameter
Aluminum
MQ(FCC_A1&AL,AL:VA;0) = −126,719+R*T*LN(1.08E−5)
MQ(FCC_A1&AL,ZN:VA;0) = −83,255+R*T*LN(1.4E−5)
MQ(CPH_A3&AL,AL:VA;0) = −79,790+R*T*LN(2.38E−5) (pe)
MQ(CPH_A3&AL,AL:VA;0) = −73,360+R*T*LN(1.08E−5) (pa)
MQ(CPH_A3&AL,ZN:VA;0) = −98,190+R*T*LN(2.84E−5) (pe)
MQ(CPH_A3&AL,ZN:VA;0) = −91,760+R*T*LN(1.29E−5) (pa)
Zinc
MMQ(FCC_A1&ZN,AL:VA;0) = −120,033+R*T*LN(2.43E−5)
MQ(FCC_A1&ZN,ZN:VA;0) = −76,569+R*T*LN(3.14E−5)
MQ(CPH_A3&ZN,AL:VA;0) = −79,790+R*T*LN(2.38E−5) (pe)
MQ(CPH_A3&ZN,AL:VA;0) = −73,360+R*T*LN(1.08E−5) (pa)
MQ(CPH_A3&ZN,ZN:VA;0) = −98,190+R*T*LN(2.84E−5) (pe)
MQ(CPH_A3&ZN,ZN:VA;0) = −91,760+R*T*LN(1.29E−5) (pa)
Interaction parameter
Aluminum
MQ(FCC_A1&AL,AL,ZN:VA;0) = 30,169−111.8*T
MQ(FCC_A1&AL,AL,ZN:VA;1) = 11,835+39.0*T
Zinc
MQ(FCC_A1&ZN,AL,ZN:VA;0) = −40,720+31.7*T
MQ(FCC_A1&ZN,AL,ZN:VA;1) = 147,763−133.7*T

pe, perpendicular to the hexagonal *c*-axis; pa, parallel with the hexagonal *c*-axis

Agren,[14] in their DICTRA study of the Ni-Cr-Al alloys, made use of the Al self-diffusion data of Legzdina and Parthasarcthy,[32] who in fact attribute the results to the early high-temperature experiments of Lundy and Murdock.[28] However, a composite view over the entire temperature range of all data suggests that a smaller frequency factor is likely to be more realistic. In contrast, no remarkable discrepancy is found for the self-diffusion of Zn among the available experimental resources; rather, all of them revealed the diffusion of Zn parallel to the hexagonal *c*-axis is larger than that perpendicular to the *c*-axis.

2.2.3 Chemical Diffusion Coefficient. Early results obtained by Hilliard et al.[15] indicate that the chemical diffusion coefficient changes slightly with increasing the Zn content in the temperature range 300 to 440 °C. Minamino et al.[37] published experimental values up to the higher temperature of 535 °C by the diffusion couple technique and Matano method. Though their data appear to be comparatively scattered, the same concentration tendency was confirmed. The last chemical diffusion coefficient measurement by Hagenschulte and Heuman[38] was accomplished by extracting data from a Boltzmann-Matano evaluation of the penetration profile; however, a comparison indicates this set of data does not extrapolate to the proper tracer diffusivity of Zn and was therefore excluded from the present assessment.

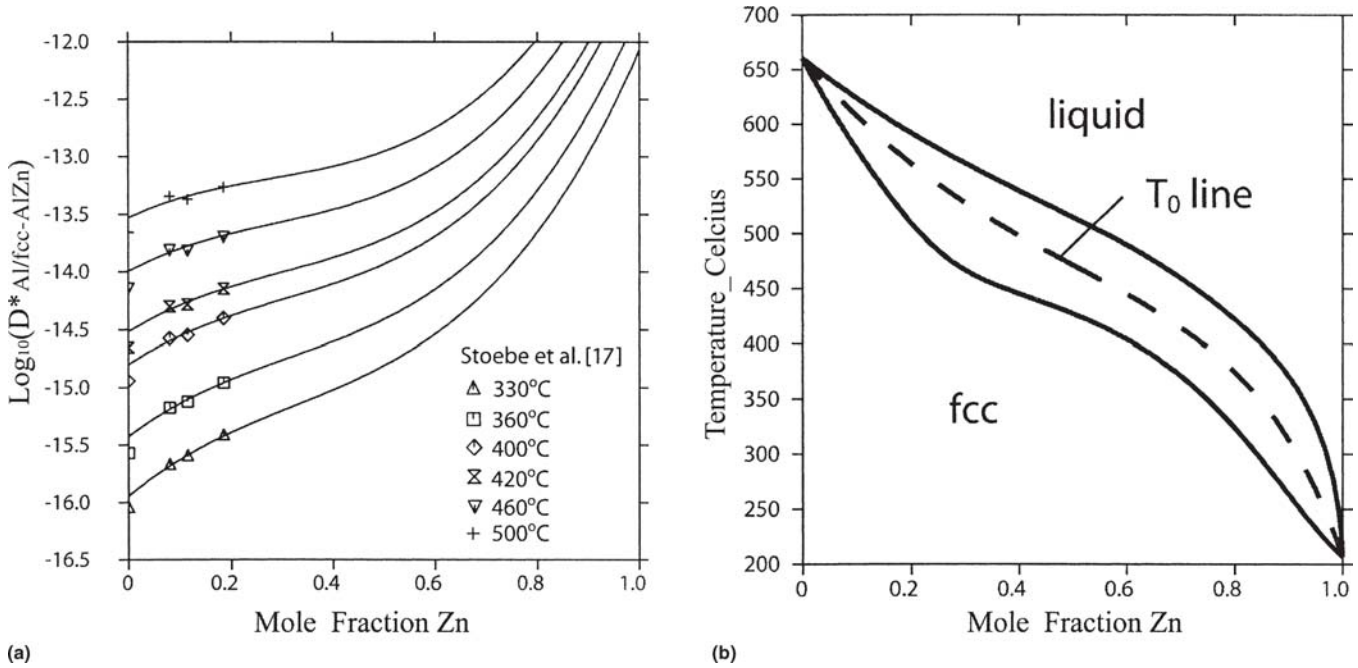

Fig. 4 (a) Tracer diffusivity of Al in the fcc solid solution at temperatures 330, 360, 400, 420, 460, and 500 °C. The solid lines are calculated. (b) The metastable isomorphous Al-Zn binary phase diagram superimposed with the T_0 line

3. Results and Simulated Diffusion Experiments

The assessment of mobility parameters was carried out with the DICTRA software by an iterative computation based on minimization of the residuals between the measured and calculated values. This section refers to the determination of necessary parameters and present results for three simulated diffusion experiments.

3.1 Self-Diffusions for Al and Zn

The calculated self-diffusion of the fcc-Al is shown in Fig. 2 by the broken line with the relevant experimental points shown for comparison. Note that in fitting to the experimental data over a much wider temperature range,[17,28-31] one obtains smaller Q_B and M_B^0 than those of Lundy and Murdock[28] and therefore derives much larger self-diffusion coefficients at low temperature (see the dotted line in Fig. 2 for comparison). Quite reasonable fits to the experimental self-diffusion data for hexagonal close-packed (cph)-Zn,[33-35] were found for both parallel and perpendicular to the hexagonal axis. This is presented in Fig. 3. It follows from Eq 2 that a self-diffusion description in hypothetical fcc-Zn and cph-Al phases are also required. The semiempirical self-diffusion relations raise the possibility of estimating these theoretical properties. An early relation proposed by Askill is often used in the DICTRA code,[39] that is:

$$Q_B = RT_m(K + 1.5V) \quad \text{(Eq 4a)}$$

$$D_0 = 1.04 \times 10^{-3} Q_B a^2 \quad \text{(Eq 4b)}$$

where K denotes the crystal structure factor, V is the valence, and a is the lattice constant. Recently, a more complex method has been suggested;[40] however, by a way of comparison, the parameters yielded from Eq 4(a) and (b) are found to behave in better accord with other parameters obtained by direct fitting of experimental points. Moreover, the relations require fewer hypothetical properties as input. On this basis, Eq 4 was used in the present work. With the melting temperature $T_m = 480$ K for the fcc-Zn being derived from the work of Mey,[5] and the lattice parameter $a = 3.939$ Å being taken from an ab initio calculation,[41] Q_B and D_0 for the fcc-Zn are yielded to be −76.6 kJ/mol and 0.314 cm^2/s, respectively. All the parameters obtained in the present work are summarized in Table 3; note that the impurity diffusivity of Al in the hypothetical fcc-Zn state was estimated by assuming its deviation from the fcc-Al self-diffusivity to be proportional to that of Zn in the fcc-Al from the fcc-Zn self-diffusivity.

Similarly, with $T_m = 550$ K and $a = 2.870$ Å,[41] Q_B and D_0 are found to be −79.8 kJ/mol and 0.238 cm^2/s for the cph-Al perpendicular to the hexagonal c-axis; however, parametric values parallel with the c-axis follow a different approximation. In this case, it is assumed that the difference of cph-Al self-diffusion between perpendicular to and parallel with the c-axis is in proportion to that of the cph-Zn; this assumption enables both values to be roughly estimated as $Q_B = -73.4$ kJ/mol and $D_0 = 0.108$ cm^2/s, and these correspond to self-diffusivities shown by the broken lines in Fig. 3.

3.2 Tracer Diffusivities in Pure Al and Al-Zn

The solid line in Fig. 2 shows the calculated Arrhenius plot of the tracer diffusivity of Zn in the pure fcc-Al, to-

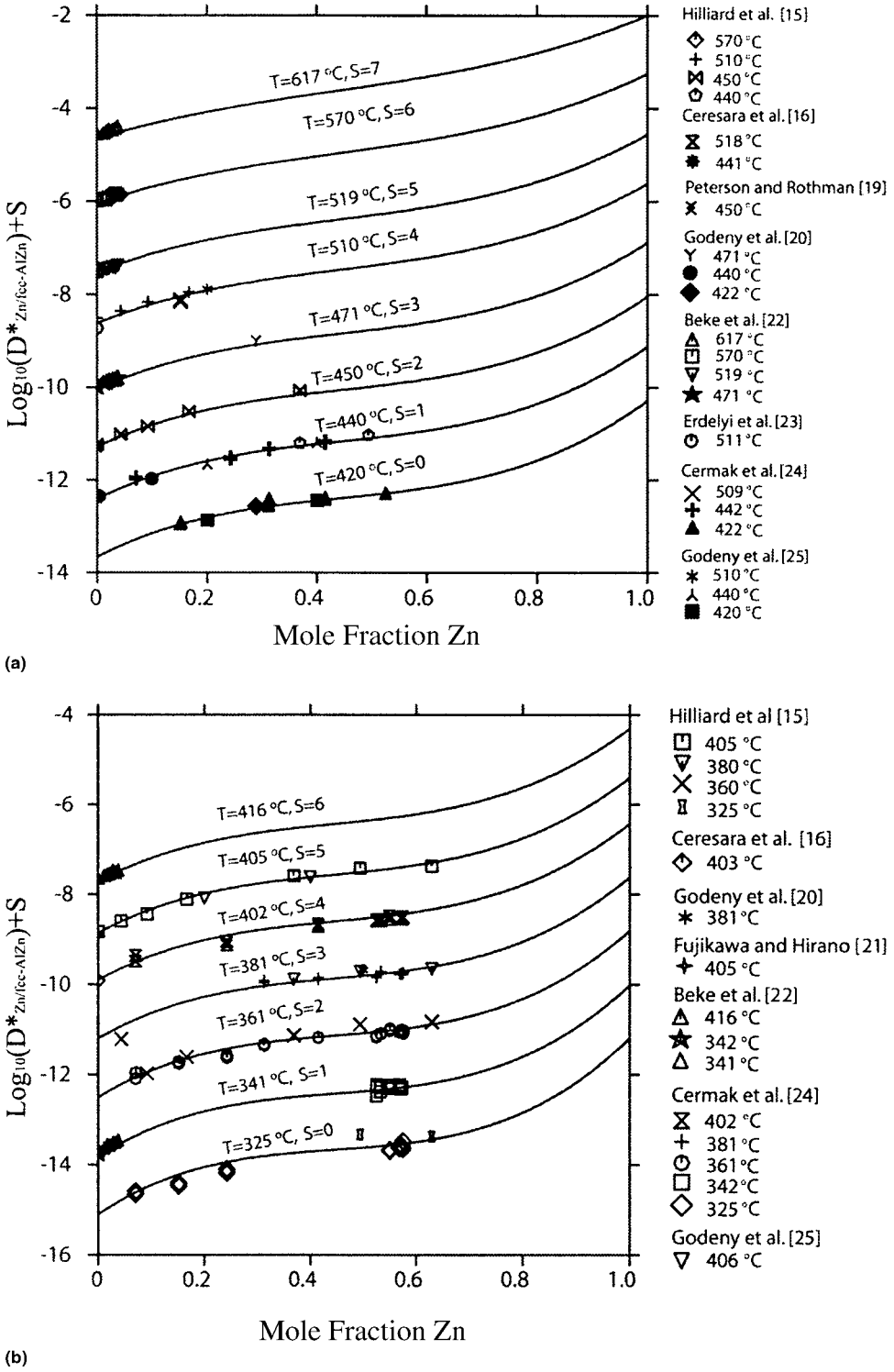

Fig. 5 The tracer diffusivity of Zn in the fcc solid solution over the temperature ranges of (a) 420-617 °C and (b) 325-416 °C. *S* is arbitrarily chosen scaling factors to separate the data at different temperatures. Without its inclusion, most of the curves and markers would lie too closely to distinguish clearly.

gether with the experimental points,[15,16,19,21-23,26,27,42,43] see the black markers therein. The fitted line reconciles very well with most of the experimental points. The calculated rate of Al tracer diffusion is shown to be dependent on Zn content in Fig. 4(a), which is in excellent agreement with the experimental data.[17] The rate is enhanced by the increase of Zn content, and the lower temperature the greater the rate of enhancement.

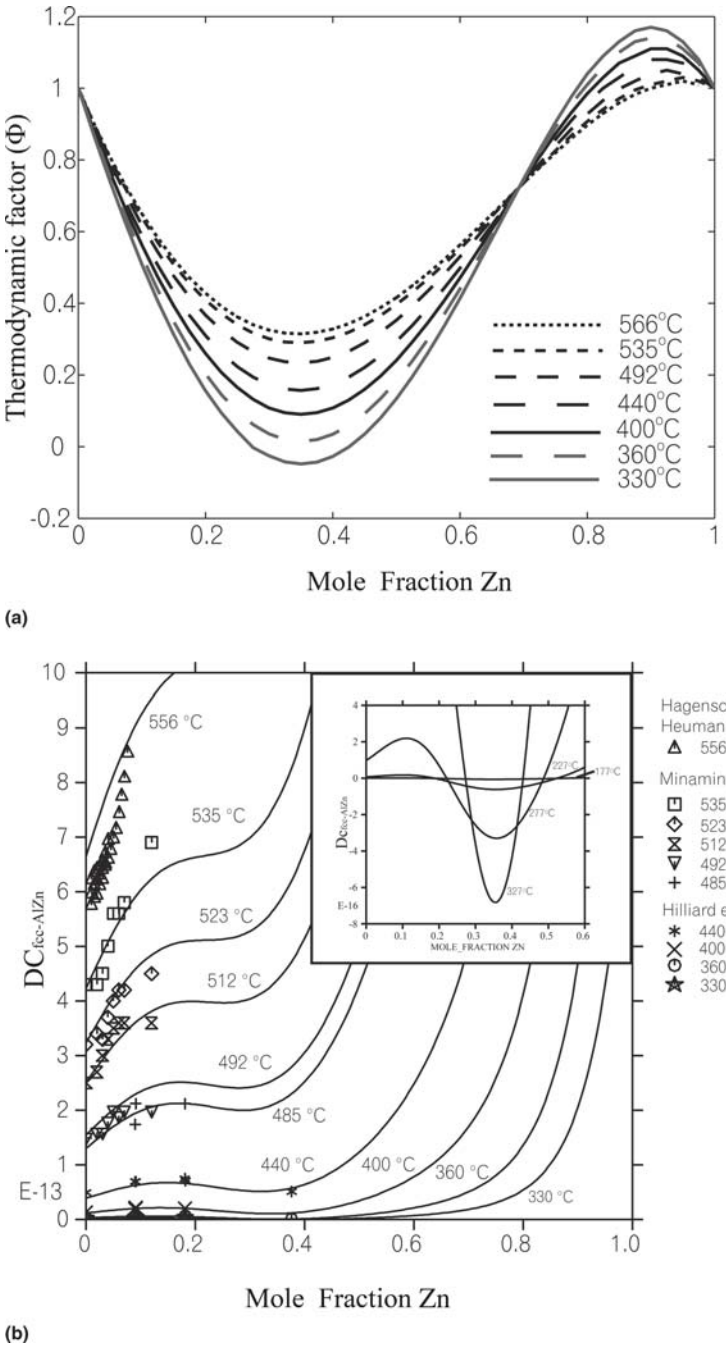

Fig. 6 (a) The calculated thermodynamic factor. (b) Comparison between calculated chemical diffusion coefficients (solid lines) and experimental data in the fcc solid solution

It is now useful to look at phase diagram information to gain a new perspective on the Al diffusion. As reviewed in Shewmon,[44] the diffusion coefficient across a binary phase diagram can be empirically estimated in such a way that adding the solute increases the diffusion coefficient in the case when the solute lowers the melting temperature of the solvent, and vice versa. Roughly speaking, the estimated diffusion coefficient tends to behave in a manner inverse to the T_0 line of the binary phase diagram. One can readily see this correspondence by a comparison between the predicted concentration dependent Al tracer diffusivity (Fig. 4a) and the metastable isomorphous liquid/fcc Al-Zn equilibrium superimposed over the T_0 line (Fig. 4b). Appreciable care was given to the calculation of the concentration dependence of the tracer diffusivity of Zn in the binary fcc solid solution. The results are presented separately in Fig. 5(a) and (b) for two temperature spans: (a) 420 to 617 °C and (b) 325 to 416 °C to include the extensive data clearly. Precise agreement, observed between the calculation and measurements, appropriately shows an S-shaped increase of Zn

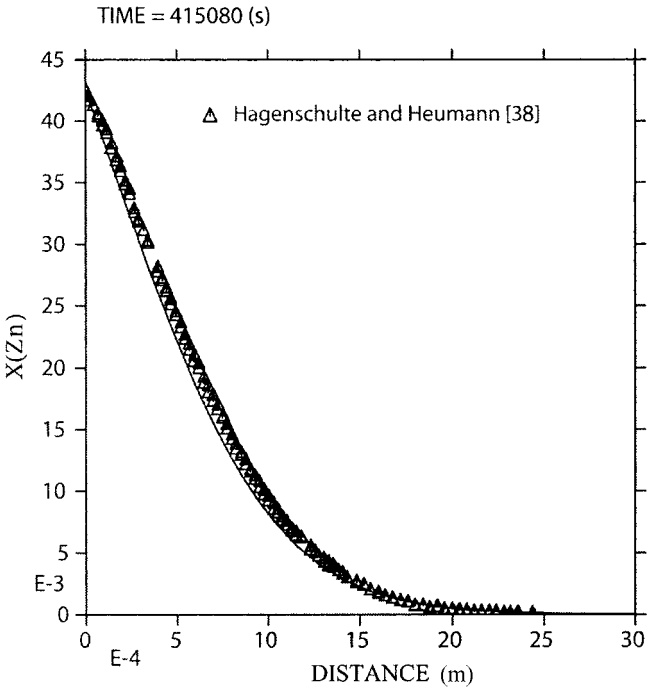

Fig. 7 Comparison between the calculated penetration profile (solid line) and the experimental data in the semi-infinite vapor-solid couple annealing at 556 °C for 115.3 h

tracer diffusivity with increased Zn concentration. This shape also exhibits inverse to that of the T_0 line of Fig. 4(b).

3.3 Chemical Diffusion Coefficient

The thermodynamic factor for diffusion, which is defined by:

$$\Phi = \frac{x_i}{RT}\frac{\partial \mu_i}{\partial x_i}$$

(μ_i is the chemical potential of species i) for the binary system, can be calculated directly from the Gibbs free energy of the fcc solid solution, as shown in Fig. 6(a). A comparison of the calculated chemical diffusion coefficient with the experimental values[15,38,45] is shown in Fig. 6(b). The figure shows that the calculated values based on the data of Fig. 4(a) seldom differ greatly from the measured points at low temperature, particularly not in the region of low Zn content. Because the difference between calculated and observed chemical diffusion coefficients are greatest for the results of Hagenschulte and Heuman[38] at 556 °C, those results are singled out for a more detailed examination in the next section.

3.4 Simulations of the Diffusion Experiments

To seek the experimental verification, the authors conducted three simulations of the penetration profile under different experimental conditions. The first example describes the semi-infinite vapor-solid diffusion couple constructed by Hagenschulte and Heumann.[38] The calculation (Fig. 7) is in remarkable agreement with the measured concentration curve. This implicitly confirms the statement by those authors that the penetration of Zn atoms is nearly unaffected by the surface oxide layer in the vapor-solid

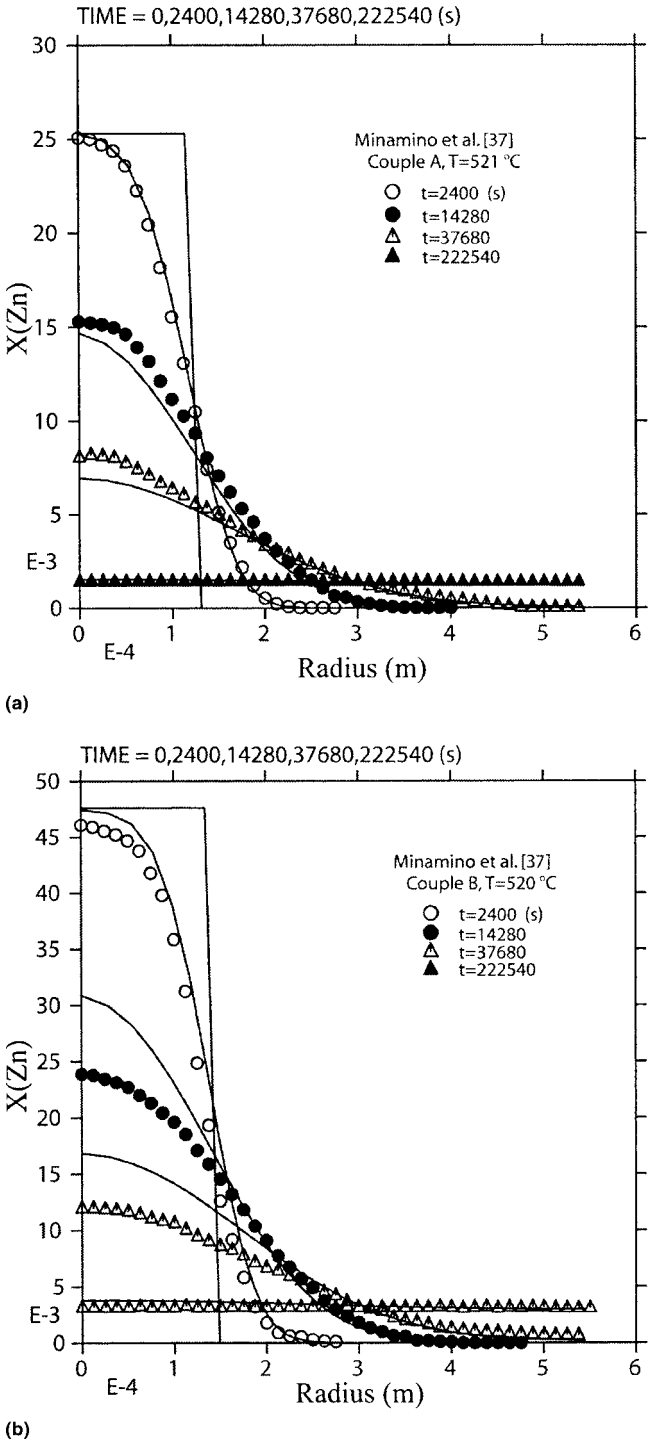

Fig. 8 Comparisons between the calculated penetration profiles (solid lines) and the experimental data in the long cylindrical diffusion couples. (a) Couple A (Al/Al-2.53at.%Zn) at 521 °C. (b) Couple B (Al/Al-4.76at.%Zn) at 520 °C

experiment. However, questions arise about their chemical diffusion data in view of the fact their data do not extrapolate to the proper tracer diffusion rate of Zn in Al and the poor agreement between them and the authors' calculation at high temperature shown in Fig. 6(b). It may be anticipated that a serious systematic error was encountered when their original concentration data were used to evaluate the diffusion rate. Figure 8 displays two Al/AlZn cylindrical diffusion couple experiments,[37] wherein the couple A was assembled with Al/Al-2.53at.%Zn annealed at 521 °C (Fig. 8a) and the couple B was with Al/Al-4.76at.%Zn annealed at 520 °C (Fig. 8b). Reasonable representation is achieved for both cases at either short or very long diffusion times, but the discrepancy is appreciable for intermediate diffusion times. Such effect becomes more pronounced for couple B. The authors believe that this discrepancy has its root in the conversion process between different profiles by the authors because the same discrepancy can also be noted in the data of Minamino et al.[37]

4. Conclusions

The diffusion mobility in the Al-Zn solid solutions is assessed by fitting to the extensive experimental data in the context of the DICTRA code. Good agreement is obtained from comprehensive comparisons made between the authors' calculations and those from different experimental resources. The assessed mobility is further validated by three successful simulations of diffusion-couple experiments.

Acknowledgment

The authors gratefully acknowledge the 21st century COE program for financial support.

References

1. A. Costa de Silva, R.R. Avillez, and K. Marques, A Preliminary Assessment of the Zn-rich Corner of the Al-Fe-Zn System and Its Implications in Steel Coating, *Z. Metallkd.,* 1999, **90**(1), p 38-43
2. X.P. Su, N.Y. Tang, and J.M. Toguri, Thermodynamic Evaluation of the Fe-Zn system, *J. Alloys Compd.,* 2001, **325**(1-2), p 129-136
3. G. Reumont, P. Perrot, J.M. Fiorani, and J. Hertz, Thermodynamic Assessment of the Fe-Zn System, *J. Phase Equilibria,* 2000, **21**(4), p 371-378
4. S.L. Chen and Y.A. Chang, A Thermodynamic Analysis of the Al-Zn System and Phase-Diagram Calculation, *Calphad,* 1993, **17**(2), p 113-114
5. S. Mey, Reevaluation of the Al-Zn System, *Z. Metallkd.,* 1993, **84**(7), p 451-455
6. Y. Du, Y.A. Chang, B. Huang, W. Gong, Z. Jin, H. Xu, Z. Yuan, Y. Liu, Y. He, and F.-Y. Xie, Diffusion Coefficients of Some Solutes in fcc and Liquid Al: Critical Evaluation and Correlation, *Mater. Sci. Eng. A,* 2003, **363**(1-2), p 140-151
7. T. Miyazaki, T. Koyama, and T. Kozakai, Computer Simulations of the Phase Transformation in Real Alloy Systems Based on the Phase Field Method, *Mater. Sci. Eng. A,* 2001, **312**(1-2), p 38-49
8. J.Z. Zhu, L.-Q. Chen, J. Shen, and V. Tikare, Coarsening Kinetics from a Variable-Mobility Cahn-Hilliard Equation: Application of a Semi-Implicit Fourier Spectral Method, *Phys. Rev. E,* 1999, **60**(4), p 3564-3572
9. J.Z. Zhu, Z.K. Liu, V. Vaithyanathan, and L.-Q. Chen, Linking Phase-Field Model to CALPHAD: Application to Precipitate Shape Evolution in Ni-Base Alloys, *Scr. Mater.,* 2002, **46**(5), p 401-406
10. J.Z. Zhu, T. Wang, A.J. Ardell, S.H. Zhou, Z.K. Liu, and L.-Q. Chen, Three-Dimensional Phase-Field Simulations of Coarsening Kinetics of γ' Particles in Binary Ni-Al Alloys, *Acta Mater.,* 2004, **52**(9), p 2837-2845
11. J.O. Andersson and J. Agren, Models for Numerical Treatment of Multicomponent Diffusion in Simple Phases, *J. Appl. Phys.,* 1992, **72**(4), p 1350-1355
12. B. Jonsson, Ferromagnetic Ordering and Diffusion of Carbon and Nitrogen in bcc Cr-Fe-Ni Alloys, *Z. Metallkd.,* 1994, **85**(7), p 498-501
13. B. Jonsson, Assessment of the Mobility of Carbon in fcc C-Cr-Fe-Ni Alloys, *Z. Metallkd.,* 1994, **85**(7), p 502-509
14 A. Engstrom and J. Agren, Assessment of Diffusional Mobilities in Face-Centered Cubic Ni-Cr-Al Alloys, *Z. Metallkd.,* 1996, **87**(2), p 92-97
15. J.E. Hilliard, B.L. Averbach, and M. Cohen, Self and Interdiffusion in Aluminum-Zinc Alloys, *Acta Metall.,* 1959, **7**(2), p 86-92
16. S. Ceresara, T. Federighi, and F. Pieragostini, Determination of Diffusion Coefficients in Metals by a Resistometric Method-Application to the Diffusion of Zn in Al, *Phys. Stat. Sol.,* 1966, **16**(2), p 439-447
17. T.G. Stoebe, R.D. Gulliver II, T.O. Ogurtani, and R.A. Huggins, Nuclear Magnetic Resonance Studies of Diffusion of Al^{27} in Aluminum and Aluminum Alloys, *Acta Metall.,* 1965, **13**(7), p 701-708
18. A. Chatterjee and D.J. Fabian, Self-Diffusion of Zinc in Aluminum and Aluminum-Zinc Alloys, *Scr. Metall.,* 1970, **4**(4), p 285-289
19. N.L. Peterson and S.J. Rothman, Impurity Diffusion in Aluminum, *Phys. Rev. B,* 1970, **1**(8), p 3264-3273
20. I. Godeny, D. Beke, F.J. Kedves, and G. Groma, Diffusion of 65Zn in Al-Zn Solid Solutions, *Phys. Stat. Sol. (a).,* 1975, **32**(1), p 195-202
21. S. Fujikawa and K. Hirano, Diffusion of ^{65}Zn in Aluminum and Al-Zn-Mg Alloy over a Wide Range of Temperature, *Trans. JIM,* 1976, **17**(12), p 809-818
22. D. Beke, I. Godeny, and F.J. Kedves, Diffusion of ^{65}Zn in Dilute AlZn, AlMg, AlZnMg and AlZnFe Alloys, *Acta Metall.,* 1977, **25**(5), p 539-550
23. G. Erdelyi, D.L. Beke, F.J. Kedves, and I. Godeny, Determination of Diffusion Coefficients of Zn, Co, and Ni in Aluminum by a Resistometric Method, *Philos. Mag. B,* 1978, **38**(5), p 445-462
24. J. Cermak, K. Ciha, and J. Kucera, Diffusion of Zn-65 in Al-Zn Solid-Solutions, *Phys. Stat Sol.,* 1980, **62**(2), p 467-474, (a)
25. I. Godeny, D.L. Beke, F.J. Kedves, and G. Groma, Diffusion of ^{65}Zn in Al-rich Heterogeneous AlZn Alloys, *Z. Metallkd.,* 1981, **72**(2), p 97-101
26. A.W. Nicholls and I.P. Jones, Determination of Low Temperature Volume Diffusion Coefficients in an Al-Zn Alloy, *J. Phys. Chem. Solids,* 1983, **44**(7), p 671-676
27. S. Varadarajan and R.A. Fournelle, Low Temperature Volume Diffusion of Zinc in Aluminum, *Acta Metall. Mater.,* 1992, **40**(8), p 1847-1854
28. T.S. Lundy and J.F. Murdock, Diffusion of Al-26 and Mn-54 in Aluminum, *J. Appl. Phys.,* 1962, **33**(5), p 1671-1673
29. P.M. Beyeler and Y. Adda, Determination of Activation Vol-

umes for Diffusion pf Atoms in Gold Copper and Aluminum, *J. Phys. (Paris),* 1968, **29**(4), p 345-352
30. R. Messer, S. Dais, and D. Wolf, Detection of Vacancy-Induced Self-Diffusion by Rotating-Frame Spin-Lattice Relaxation in Aluminum, *Proc. 18th Ampere Congress* (Nottingham, England), 1974, P.S. Allen, E.R. Andrew, and C.A. Bates, Ed., Nottingham, England, North-Holland Publishing, Amsterdam, 1975, p 327-328
31. T.E. Volin and R.W. Balluffi, Annealing Kinetics of Voids and Self-Diffusion Coefficient in Aluminum, *Phys. Stat. Sol.,* 1968, **25**(1), p 163-173
32. D. Legzdina and T.A. Parthasarcthy, Deformation Mechanisms of a Rapidly Solidified Al-8.8Fe-3.7Ce Alloys, *Metall. Trans. A,* 1987, **18A**(10), p 1713-1719
33. G.A. Shirn, E.S. Wajda, and H.B. Huntington, Self-Diffusion in Zinc, *Acta Metall.,* 1953, **1**(5), p 513-518
34. A.P. Batra, Anisotropic Isotope Effect for Diffusion of Zinc and Cadmium in Zinc, *Phys. Rev.,* 1967, **159**(3), p 487-499
35. N.L. Peterson and S.J. Rothman, Isotope Effect in Self-Diffusion in Zinc, *Phys. Rev.,* 1967, **163**(3), p 645-649
36. L.C. Chhabildas and H.M. Gilder, Thermal Coefficient of Expansion of an Activated Vacancy in Zinc from High-Pressure Self-Diffusion Experiments, *Phys. Rev. B,* 1972, **5**(6), p 2135-2144
37. Y. Minamino, T. Yamane, and K. Tokuda, Interdiffusion in Al-Zn Measured by the Electric Resistance, *Z. Metallkd.,* 1980, **71**(2), p 90-95
38. H. Hagenschulte and T.H. Heuman, Diffusion, the Kirkendall Effect and Vacancy Jump Frequency Ratios in Dilute Al-Zn Alloys, *J. Phys.: Condens. Matter,* 1994, **6**(10), p 1985-1998
39. J. Askill, *Tracer Diffusion Data for Metals, Alloys and Simple Oxides,* IFI, Plenum, 1970, p 19-26
40. A.V. Gorshkov, Relation for the Self-Diffusion Parameters of Elemental Substances, *Inorg. Mater.,* 2000, **36**(7), p 688-690
41. Y. Wang, S. Curtarolo, C. Jiang, R. Arroyave, T. Wang, G. Ceder, L.-Q. Chen, and Z.-K. Liu, Ab initio Lattice Stability in Comparison with CALPHAD Lattice Stability, *Calphad,* 2004, **28**(1), p 79-90
42. A. Fontell, E. Arminen, and M. Turunen, Application of Backscattering Method for Measurement of Diffusion of Zinc in Aluminum, *Phys. Stat. Sol. (a),* 1973, **15**(1), p 113-119
43. S. Nishikawa and K. Umezu, Analysis of Penetration Data of Zn Along Random Boundaries of Pure Aluminum, *J. Jpn. Inst. Light Met.,* 1976, **26**(1), p 35-43, (in Japanese)
44. P. Shewmon, *Diffusion in Solids,* 2nd ed., The Minerals, Metals & Materials Society, 1989
45. Y. Minamino, T. Yamane, K. Tsukamoto, J. Takahashi, and H. Kimura, Interdiffusion in Al Solid Solution of Ternary Al-Ag-Zn System, *Z. Metallkd.,* 1984, **75**(12), p 943-947